European Radiology (2018) 28:2647–2654
https://doi.org/10.1007/s00330-017-5256-3

CARDIAC

Third generation dual-source CT enables accurate diagnosis of coronary restenosis in all size stents with low radiation dose and preserved image quality

Yuehua Li[1] · Mengmeng Yu[1] · Wenbin Li[1] · Zhigang Lu[2] · Meng Wei[2] · Jiayin Zhang[1]

Received: 22 September 2017 / Revised: 5 December 2017 / Accepted: 18 December 2017 / Published online: 18 January 2018

Abstract

Objectives To investigate the diagnostic performance of low dose stent imaging in patients with large (≥ 3 mm) and small (< 3 mm) calibre stents by third-generation dual-source CT.

Methods Symptomatic patients suspected of having in-stent restenosis (ISR) were prospectively enrolled. Coronary computed tomography angiography (CCTA) and invasive coronary angiography (ICA) were performed within 1 month for correlation. Binary ISR was defined as an in-stent neointimal proliferation with diameter stenosis ≥ 50%. The radiation dose and image quality of CCTA were also assessed.

Results Sixty-nine patients with 140 stents were ultimately included for analysis. The mean total radiation dose of CCTA was 1.3 ± 0.72 mSv in all patients and 0.95 ± 0.17 mSv in patients with high pitch acquisition. The overall diagnostic accuracy of CCTA stent imaging of patient-based, lesion-based and stent-based analysis was 95.7%, 94.1% and 94.3%, respectively. Further, the diagnostic accuracy of CCTA in the small calibre stent group (diameter < 3 mm) was slightly lower than that of the large calibre stent group (diameter ≥ 3 mm) (88.5% versus 98.7%, p = 0.01).

Conclusions Third-generation dual-source CT enables accurate diagnosis of coronary ISR of both large and small calibre stents. Low radiation dose could be achieved with preserved image quality.

Key Points

- *Third-generation DSCT enables accurate diagnosis of coronary ISR of all size stents.*
- *Low radiation dose could be achieved with preserved image quality.*
- *The diagnostic accuracy of CCTA of small calibre stents was 88.5%.*

Keywords Coronary artery disease · Multidetector computed tomography · Angiography · Stents · Percutaneous coronary intervention

Dr. Yuehua Li and Dr. Mengmeng Yu contributed equally to this study.

Electronic supplementary material The online version of this article (https://doi.org/10.1007/s00330-017-5256-3) contains supplementary material, which is available to authorized users.

✉ Jiayin Zhang
andrewssmu@msn.com

[1] Institute of Diagnostic and Interventional Radiology, Shanghai Jiao Tong University Affiliated Sixth People's Hospital, #600, Yishan Rd, Shanghai 200233, China

[2] Department of Cardiology, Shanghai Jiao Tong University Affiliated Sixth People's Hospital, #600, Yishan Rd, Shanghai, China

Abbreviations

CCTA	Coronary computed tomography angiography
ICA	Invasive coronary angiography
ISR	In-stent restenosis

Introduction

Coronary artery stenting is currently the predominant strategy of myocardial revascularization in patients with obstructive coronary artery disease [1, 2]. Even with the wide application of drug-eluting stent (DES), in-stent restenosis (ISR) and stent occlusion remain the major complications of this procedure [3, 4].

Coronary computed tomography angiography (CCTA) has been established as a useful non-invasive imaging modality for diagnosis of ISR and revealed to have high diagnostic accuracy for evaluation of large calibre stents (diameter ≥ 3 mm) when compared to invasive coronary angiography (ICA) [5–7]. However, the visualization of stent lumen by CCTA is markedly impaired in patients with small calibre stents [8]. With the recent introduction of third-generation dual-source CT, assessment of small calibre stents was reported to be technically feasible at low radiation dose level in ex vivo phantom studies [9–11]. Therefore, we aimed to investigate the diagnostic performance of in vivo low dose stent imaging in patients with large and small calibre stents by third-generation dual-source CT, with reference to ICA.

Methods

Patient population

Between November 2016 and April 2017, consecutive symptomatic post-stenting patients, who were suspected of having ISR, were prospectively enrolled in our study. The inclusion criteria were (1) patients presented with symptoms suggestive of ISR; (2) the details of implanted stents were known. The exclusion criteria included (1) patients refused to undergo CCTA prior to ICA; (2) patients did not undergo CCTA and ICA within 1 month; (3) the details of implanted stents were unknown; (4) the image quality of CCTA was non-diagnostic. All patients gave written informed consent and the hospital ethics committee approved the study protocol.

CCTA scan protocol

A third-generation dual-source CT (SOMATOM Force, Siemens Healthcare, Forchheim, Germany) equipped with a fully integrated circuit detector system (Stellar Infinity, Siemens) was employed for scanning. A β-blocker (25–50 mg, Betaloc ZOK; AstraZeneca, China) was administrated orally 1 h prior to the examination in patients with heart rate > 70 bpm. Nitroglycerin was given sublingually in all patients. Imaging was performed by using a bolus tracking technique, with regions of interest placed in the ascending aorta. A bolus of contrast media (Iopamidol, 370 mg iodine/ml, Schering AG, Berlin, German) was injected into an antecubital vein at the rate of 4–5 ml/s, followed by a 40-ml saline flush by using a dual-barrel power injector (Tyco, Cincinnati, USA). The amount of the contrast medium was determined according to the patient's body weight and details are given in the online supplement Table 1. Prospective ECG-triggered high pitch helical acquisition (Flash mode) was performed in patients with final heart rate < 70 bpm, with delay time = 4 s, collimation = 96 × 0.6 mm, reconstructed slice thickness = 0.75 mm, reconstructed slice interval = 0.5 mm, rotation time = 250 ms and pitch = 3.2. Prospective ECG-triggered sequential acquisition was performed in patients with final heart rate ≥ 70 bpm, with the centre of the triggering window set at 35% of the RR interval, with delay time = 2s, collimation = 96 × 0.6 mm, reconstructed slice thickness = 0.75 mm, reconstructed slice interval = 0.5 mm and rotation time = 250 ms. The automated tube voltage and current modulation (CARE KV and CAREDose 4D, Siemens) were enabled in all patients to determine the tube voltage and current according to individual body habitus. The reference tube current was set as 300 mAs and the reference tube voltage was set as 100 kVp.

Image reconstruction and analysis

For better delineation of both vessel wall and stent lumen, two sets of axial images were reconstructed with different kernels and strength levels of third-generation iterative reconstruction (IR) technique (ADMIRE, Siemens): smooth kernel (Bv40, strength 3) and sharp kernel (Bv44, strength 4). Data was transferred to an offline workstation (SyngoVia, Siemens) for further analysis. Curved planar reformation (CPR) and short axis view of the stents with sharp kernel reconstruction were used for evaluation of ISR, whereas images with smooth kernel reconstruction were used for assessment of native coronary arteries [12]. All images were evaluated independently by two radiologists experienced in CCTA who were blinded to the number, location, diameter and type of stents and to the clinical patients' history. Disagreements between the two readers for any image set were resolved by consensus, and the consensus findings were used in all assessments of diagnostic performance.

Subjective image quality of patients was assessed by using a 3-point semi-quantitative scale [8]: 3 = excellent (absence of artefact), 2 = acceptable (presence of less artefact, but still diagnostic), 1 = poor (presence of severe artefact, non-diagnostic). CT attenuation and image noise (defined as the standard deviation of CT density in a region of interest) of the aortic root and proximal coronary arteries, signal-to-noise ratio (SNR) and contrast-to-noise ratio (CNR) were evaluated as objective parameters of image quality, as previously described [13]. For CCTA attenuation and image noise, a circular region of interest (ROI) was placed in the aortic root at the level of the left main coronary artery ostium (2.5 cm in diameter) as well as in the proximal segments of the left and right coronary arteries (as large as possible with exclusion of vessel wall). All regions of interests were measured three times, and mean measurements were used for statistical analysis. The SNR was calculated as the mean HU divided by the mean image noise measured in the corresponding vessels. The proximal vessel contrast was defined as the difference between the CT attenuation of the vessel lumen and the surrounding tissue immediately next to the vessel contour. The CNR was calculated by

dividing that vessel contrast values by image noise of the corresponding vessel.

Binary ISR is considered as an in-stent neointimal proliferation with diameter stenosis ≥ 50%. According to Mehran classification, the angiographic patterns of binary ISR were further classified by CCTA into four types [14]: focal, diffuse intrastent, diffuse proliferative and total occlusion. The angiographic patterns of neointimal proliferation were also similarly classified into two types: focal (≤ 10 mm) and diffuse (>10 mm). If coronary stents or vessels were rated unassessable (image quality score 1), they were considered positive (presence of significant coronary stenosis). Subsequently, results of CCTA were compared with those of the ICA. Native obstructive coronary lesions located on the vessels with diameter ≥ 1.5 mm were also recorded and compared to ICA findings for patient-based analysis.

ICA procedure and analysis

The ICA was performed with standard techniques, and at least two different views were obtained for each main vessel. All segments were evaluated by two skilled observers who were blinded to the results of CCTA. Disagreements between the two readers were resolved by consensus. Angiographic binary restenosis was defined as luminal stenosis > 50% occurring within stents by visual assessment and the angiographic patterns were classified into four types, employing the same grading system as for CCTA. Balloon angioplasty or stent implantation was performed for treatment of ISR. De novo lesions with significant progression were also treated with stent implantation when they were considered as the culprit lesions responsible for patients' recurrent symptoms.

Statistical analysis

Statistical analysis was performed using commercially available statistical software (SSPS, V13.0, SPSS Inc., Chicago, USA). One-sample Kolmogorov–Smirnov test was used to check the assumption of normal distribution. Quantitative variables with normal distribution were expressed as mean ± standard deviation (SD) while median and quartiles were used otherwise. The *t* test and Pearson test were used for normally distributed data while the Mann–Whitney *U* test was used for data that were not normally distributed. The chi-square test was used to compare proportions. The diagnostic accuracy was evaluated by sensitivity, specificity, positive predictive value (PPV) and negative predictive value (NPV). Interobserver agreement was expressed in Cohen's kappa value (κ) for categorical variables. A probability value of $p < 0.05$ was considered to be statistically significant.

Results

Clinical characteristics

A total of 83 symptomatic patients suspected for ISR were initially enrolled. Six patients refused to undergo CCTA prior to ICA and were excluded. Five patients were excluded because of unknown details of previous implanted stents. Three patients were excluded because the interval between CCTA and ICA was longer than 1 month (Fig. 1). Notably, none of the patients were excluded because of non-diagnostic image quality. Therefore, 69 patients with 140 stents were finally included in the study (mean age 68.7 ± 9.8 years, range 46–87 years; 64 men [mean age 67.9 ± 9.5 years, range 46–86] and 5 women [mean age 78.6 ± 8.3 years, range 65–87], $p = 0.017$). The mean contrast medium used for CCTA was 50.6 ± 5.7 ml (range 40–60 ml). ICA was performed in 69 patients with an interval of 9.8 ± 6.5 days (range 1–29 days). Detailed demographic data are given in Table 1.

Image quality and radiation dose of CCTA

Prospective ECG-triggered high pitch helical acquisition (Flash mode) was performed in 40 patients, whereas prospective ECG-triggered sequential acquisition was employed in 29 patients. The mean total dose length product (DLP) of the whole cohort was 93.2 ± 51.1 mGy cm (range 47–273 mGy cm), corresponding to 1.3 ± 0.72 mSv (range 0.66–3.8 mSv) when using 0.014 as the conversion factor [15]. The mean

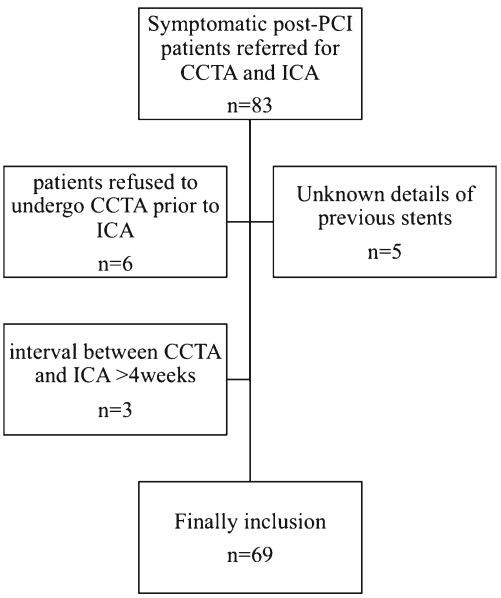

Fig. 1. Flow chart of patient inclusion and exclusion. CCTA coronary computed tomography angiography, ICA invasive coronary angiography, PCI percutaneous coronary intervention

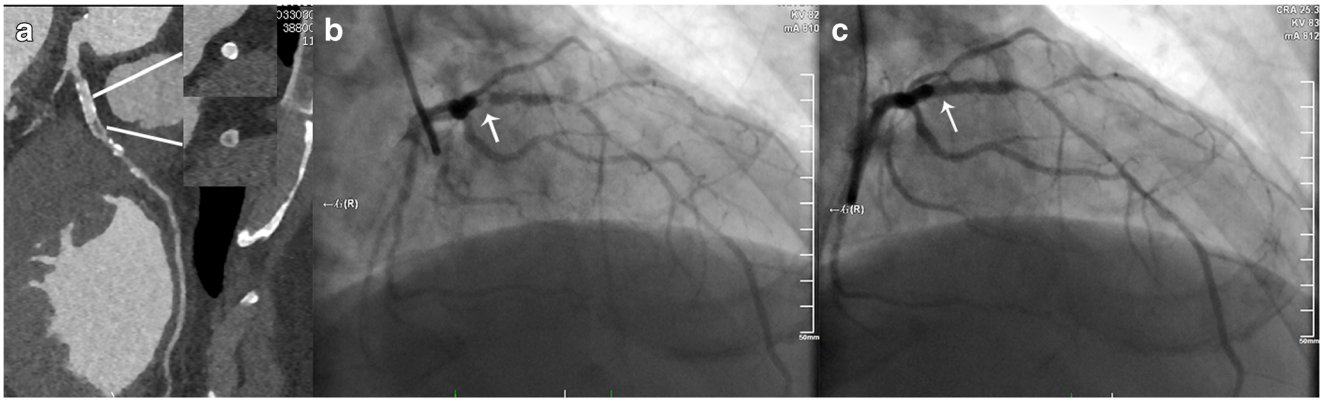

Fig. 2. CCTA-based diagnosis of ISR in a 63-year-old male patient. **a** CPR image of LAD showed focal ISR in a 2.75 mm coronary stent (Xience Prime 2.75 × 15mm, Abbott, USA). **b** ICA of left coronary artery confirmed the diagnosis of focal ISR (white arrow). **c** PCI was performed to restore the lumen patency (white arrow). CCTA coronary computed tomography angiography, CPR curved planar reformation, ICA invasive coronary angiography, ISR in-stent restenosis, LAD left anterior descending, PCI percutaneous coronary intervention

total radiation dose was markedly lower in patients with high pitch helical acquisition than in patients with sequential acquisition (0.95 ± 0.17 mSv vs. 1.8 ± 0.87 mSv, $p < 0.001$). However, the subjective image quality score, SNR and CNR were without significant difference between the two scan mode subgroups (Table 2).

Diagnostic performance of CCTA with reference to ICA

A total of 36 patients with 45 stents were diagnosed to have binary ISR according to CCTA findings. The interobserver agreement of diagnosing ISR by CCTA was good (kappa = 0.816, $p < 0.001$). The number of unassessable stents was 5 for the small calibre group and was zero for the large calibre group. Stent-based (based on each stent) and lesion-based (overlapping stents were considered as one lesion) analyses were performed to test the diagnostic performance of stent imaging. Patient-based analysis was performed to investigate the overall performance when including both stented segment as well as native obstructive coronary lesions. ICA confirmed ISR in 37 stents. Compared to ICA findings, the overall diagnostic accuracy of CCTA stent imaging of patient-based, lesion-based and stent-based analysis was 95.7%, 94.1% and 94.3%, respectively. The diagnostic performance of stent assessment was good in terms of sensitivity, specificity, PPV and NPV (Table 3, Figs. 2, 3, 4, 5). The CCTA Mehran classification was also found to be accurate (94.3%, 33/35) with reference to ICA correlation.

The diagnostic accuracy, sensitivity, specificity, PPV and NPV were all above 95% for the large calibre stent group. Those numbers were slightly lower for the small calibre stent group (Table 3). This was mainly due to the unassessable stents in the small calibre group, which resulted in relatively low specificity and PPV. The diagnostic accuracy of small stents was 92.9% (52/56) when unassessable stents were excluded. However, the overall

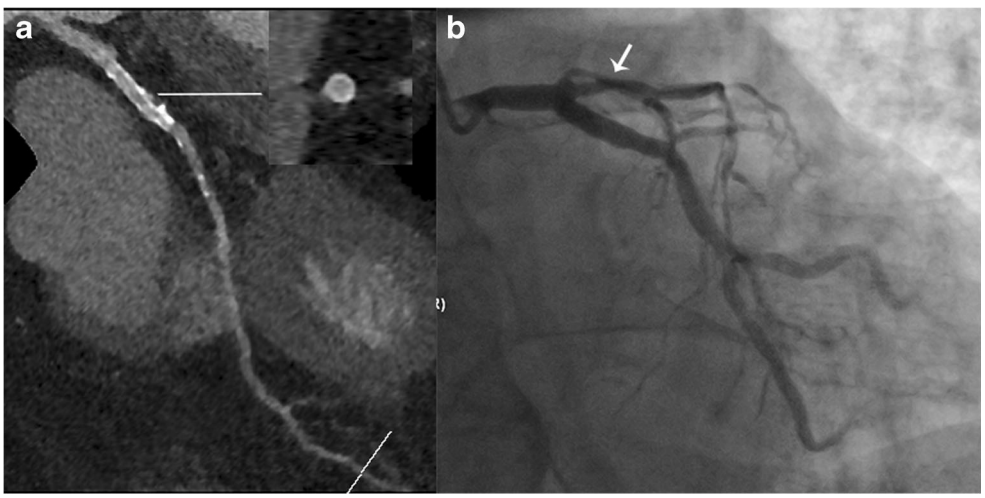

Fig. 3. CCTA-based diagnosis of patent stent in a 68-year-old male patient. **a** CPR image of LAD showed absence of ISR in a 2.75 mm coronary stent (Yinyi 2.75 × 18mm, Yinyi Biotech, China). **b** ICA of left coronary artery confirmed the stent patency (white arrow). CCTA coronary computed tomography angiography, CPR curved planar reformation, ICA invasive coronary angiography, ISR in-stent restenosis, LAD left anterior descending

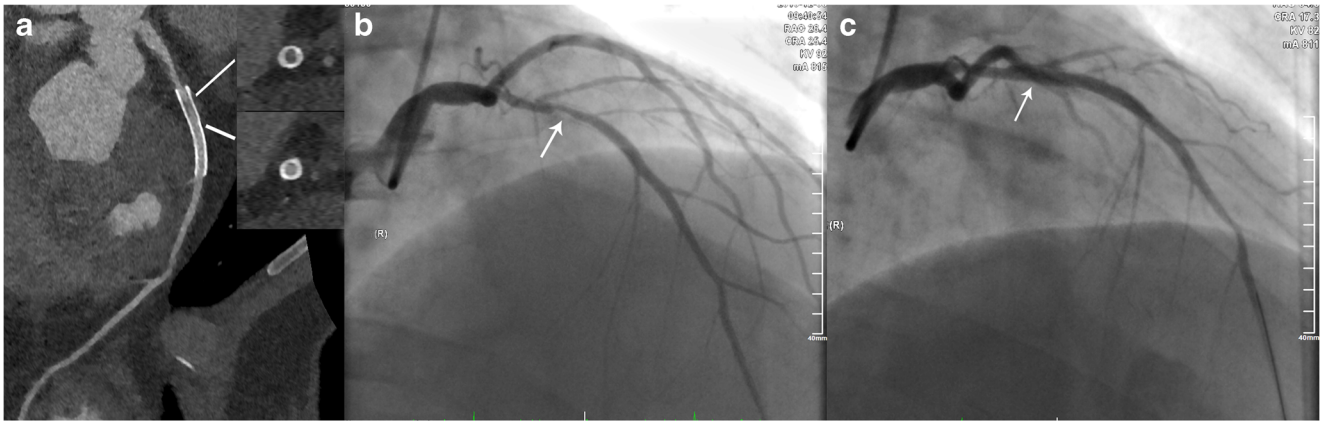

Fig. 4. CCTA-based diagnosis of ISR in a 54-year-old male patient. **a** CPR image of LAD showed diffuse ISR in a 3.5 mm coronary stent (Resolute 3.5 × 30mm, Medtronic, USA). **b** ICA of left coronary artery confirmed the diagnosis of diffuse ISR (white arrow). **c** PCI was performed to restore the lumen patency (white arrow). CCTA coronary computed tomography angiography, CPR curved planar reformation, ICA invasive coronary angiography, ISR in-stent restenosis, LAD left anterior descending, PCI percutaneous coronary intervention

accuracy of small diameter stents was over 88% for stent-based, lesion-based and patient-based analyses.

Discussion

This study revealed two main findings: (1) Third-generation dual-source CT enables accurate stent imaging in patients with both large and small calibre stents with reference to ICA. (2) The mean radiation dose of CCTA was as low as 1.3 mSv.

DES has dramatically reduced the rates of restenosis and target lesion revascularization (TLR) compared with bare-metal stents (BMS) [16]. However, a low rate of ISR after DES still exists, and its prevalence is not negligible because the population treated with DES is large. Although the majority of cases of ISR lead to recurrent symptoms, some cases are clinically silent and late myocardial infarction (MI) can be caused by highly stenotic ISR or stent occlusion [17–19]. Early detection of stent occlusion is of clinical significance to prevent secondary MI and therefore improve long-term prognosis. However, small calibre stents (diameter < 3 mm) dramatically reduce the visibility of stent lumen and subsequently lead to a large proportion of unassessable stents [7, 8]. Therefore, CCTA imaging for small calibre stents was considered as inappropriate according to an appropriate use criteria document [20].

Third-generation dual-source CT is equipped with an integrated circuit detector, which allows for a higher spatial resolution in the z direction (out-of-plane resolution) and lower image noise [21]. According to previous

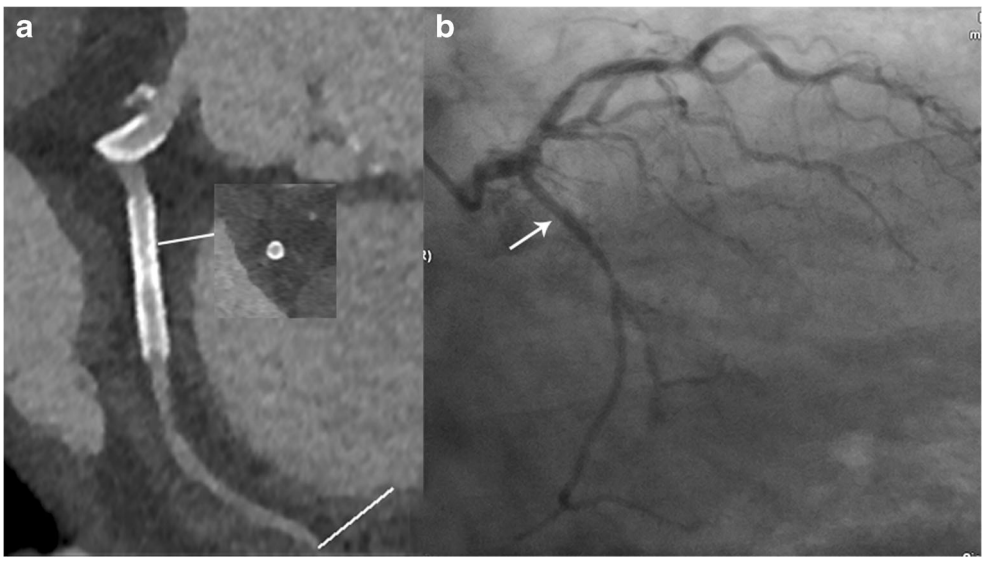

Fig. 5. CCTA-based diagnosis of patent stent in a 73-year-old male patient. **a** CPR image of LCx showed absence of ISR in a 2.5 mm coronary stent (Resolute 2.5 × 18 mm, Medtronic, USA). **b** ICA of left coronary artery confirmed the stent patency (white arrow). CCTA coronary computed tomography angiography, CPR curved planar reformation, ICA invasive coronary angiography, ISR in-stent restenosis, LCx left circumflex

Table 1 Demographic data

Population	69
Age (years)	68.7 ± 9.8
Weight (kg)	73.3 ± 8.3
BMI	23 ± 2.2
Risk factors	
Hyperlipidaemia	23 (33.3%)
Hypertension	41 (59.4%)
Smoking	24 (34.8%)
Diabetes	21 (30.4%)
Clinical presentations	
Stable angina	49 (71%)
Unstable angina	20 (29%)
Stented vessel (n = 140)	
LM	8 (5.7%)
LAD	56 (40%)
LCx	30 (21.4%)
RCA	35 (25%)
Diagonal	6 (4.3%)
OM	2 (1.4%)
Ramus intermedius	1 (0.7%)
PLV	2 (1.4%)
Stent diameter (nominal) (n = 140)	
4.0 mm	4 (2.9%)
3.5 mm	21 (15%)
3.0 mm	54 (38.6%)
2.75 mm	37 (26.4%)
2.5 mm	20 (14.3%)
2.25 mm	4 (2.9%)
Stent type	
Xience Prime (DES)	35 (25%)
Resolute (DES)	41 (29.3%)
Firebird 2 (DES)	45 (32.1%)
Yinyi (DES)	12 (8.6%)
Taxus Liberte (DES)	4 (2.9%)
Cypher Select (DES)	3 (2.1%)

BMI body mass index, *DES* drug eluting stent, *LAD* left anterior descending, *LCx* left circumflex, *LM* left main, *OM* obtuse marginal, *PLV* posterior lateral vessel, *RCA* right coronary artery

ex vivo phantom study by Gassenmaier et al., combined application of an integrated circuit detector and advanced IR enables significant improvement of stent lumen visibility [10]. In another moving heart phantom study by Geyer et al., the implementation of an integrated circuit detector provides substantially sharper out-of-plane resolution at CT of small diameter coronary artery stents, while the use of iterative reconstruction favourably contributes to improved in-plane stent visualization that is independent of stent diameter and heart rate [9]. However, validation of the above findings has not been performed by in vivo study to confirm the diagnostic accuracy in a real-world clinical setting.

In the current study, symptomatic patients with stent diameter from 2.25 mm to 4 mm were prospectively enrolled and evaluated by third-generation dual-source CT. In line with previous phantom studies, in vivo small calibre stents assessment was revealed to be feasible. Although the diagnostic performance of the small stents group was slightly inferior to that of the large stents group, the diagnostic accuracy of both groups was each above 85% with reference to ICA, whereas the unassessable stent number of the small calibre group was below 10%. Moreover, it is notable that the current result was achieved in a real-world clinical setting in patients with varied heart rates and body habitus. Therefore, it might further expand the CCTA indication for small stent imaging if this finding could be confirmed by future prospective studies with larger sample size.

In addition to the promising diagnostic performance of small calibre stent imaging by third-generation dual-source CT, sub-millisievert acquisition was also achieved in the majority of the cohort. This could be ascribed to the combined use of low tube voltage and tube current. An automated dose modulation technique was employed to determine the tube voltage and current according to the patients' habitus. More than 78% (54/69) of the patients were scanned at 80 kVp or less and only approximately 20% of patients were imaged at 90 kVp or above. With the application of advanced IR technique, it was further feasible to acquire good image quality as well as high SNR/CNR at low level of radiation dose. Thus, it enables successful small stent imaging with less radiation burden.

The major limitation of this study was the relatively small sample size of 2.25 mm stents. The 2.5 mm and 2.75 mm stents accounted for the majority of small calibre stents. Therefore, the diagnostic performance of CCTA for 2.25 mm stents remains uncertain and needs to be validated by further studies. Second, intravascular ultrasound (IVUS) was not used to measure intrastent lumen area. The head-to-head comparison of CCTA and IVUS stent measurement was consequently not available. Finally, the spectrum of stents in our study was relatively narrow and only covered six different vendors. Further studies are needed to investigate the diagnostic performance in a wider stent spectrum.

In conclusion, third-generation dual-source CT enables accurate diagnosis of coronary ISR of both large and small calibre stents. Low radiation dose could be achieved with preserved image quality.

Table 2 Image quality and radiation dose of groups with different acquisition modes

	All patients (n = 69)	Patients with high pitch acquisition (n = 40)	Patients with sequential acquisition (n = 29)	p value
Heart rate during acquisition (bpm) [a]	66 (63–73)	63.5 (62–65)	73 (72–77)	< 0.001
Volume of contrast medium (ml) [a]	50 (50–50)	50 (50–50)	50 (50–50)	0.935
Tube voltage (kVp) [a]	80 (70–80)	80 (70–87.5)	80 (70–80)	0.634
Total radiation dose (mSv) [b]	1.3 ± 0.72	0.95 ± 0.17	1.8 ± 0.87	< 0.001
Subjective image quality score [a]	3 (3–3)	3 (3–3)	3 (3–3)	0.943
SNR				
Aorta	19 ± 5.3	19.8 ± 5.9	17.8 ± 4.1	0.129
LM	18.4 ± 6.9	18.7 ± 6.7	18.1 ± 7.3	0.719
LAD	17.9 ± 6.8	18.5 ± 7.4	16.9 ± 5.8	0.335
LCx	17.7 ± 8	18 ± 9.1	17.2 ± 6.4	0.684
RCA	19.1 ± 9.4	19.7 ± 10.9	18.3 ± 7	0.542
CNR				
Aorta	21.9 ± 6	23 ± 6.7	20.3 ± 4.6	0.07
LM	21.1 ± 7.7	21.5 ± 7.3	20.6 ± 8.3	0.646
LAD	20.5 ± 7.5	21.4 ± 8.2	19.3 ± 6.1	0.258
LCx	20.5 ± 9	20.9 ± 10.1	19.8 ± 7.5	0.603
RCA	22.2 ± 10.9	23.1 ± 12.8	21 ± 7.4	0.443

CNR contrast noise ratio, *LAD* left anterior descending, *LCx* left circumflex, *LM* left main, *RCA* right coronary artery, *SNR* signal noise ratio

[a] Dates are medians, with the first to third quartile in parentheses

[b] Total radiation dose includes the radiation dose of scout image, calcium score and coronary CT angiography

Table 3 Diagnostic performance of CCTA imaging for diagnosing ISR in patients with large and small calibre stents

Accuracy	All	Large calibre stents (stent diameter ≥ 3 mm)	Small calibre stents (stent diameter < 3 mm)	p value
Patient-based analysis (n = 69) [a]				
Accuracy	95.7% (66/69)	96.9% (31/32)	94.6% (35/37)	0.643
Sensitivity	100% (57/57)	100% (27/27)	100% (30/30)	1
Specificity	75% (9/12)	80% (4/5)	71.4% (5/7)	0.735
PPV	95% (57/60)	96.4% (27/28)	93.8% (30/32)	0.635
NPV	100% (9/9)	100% (4/4)	100% (5/5)	1
Lesion-based analysis (n = 118) [b]				
Accuracy	94.1% (111/118)	98.4% (63/64)	88.9% (48/54)	0.029
Sensitivity	100% (35/35)	100% (19/19)	100% (16/16)	1
Specificity	91.6% (76/83)	97.8% (44/45)	84.2% (32/38)	0.027
PPV	83.3% (35/42)	95% (19/20)	72.7% (16/22)	0.053
NPV	100% (76/76)	100% (44/44)	100% (32/32)	1
Stent-based analysis (n = 140)				
Accuracy	94.3% (132/140)	98.7% (78/79)	88.5% (54/61)	0.01
Sensitivity	100% (37/37)	100% (22/22)	100% (15/15)	1
Specificity	92.2% (95/103)	98.2% (56/57)	84.8% (39/46)	0.011
PPV	82.2% (37/45)	95.7% (22/23)	68.2% (15/22)	0.016
NPV	100% (95/95)	100% (56/56)	100% (39/39)	1
Assessable stents	96.4% (135/140)	100% (79/79)	91.8% (56/61)	0.01

CCTA coronary computed tomography angiography, *ISR* in-stent restenosis, *NPV* negative predictive value, *PPV* positive predictive value

[a] ISR as well as native obstructive coronary lesions were both included for patient-based analysis

[b] The smallest stent diameter was recorded for lesion-based analysis of ISR with multiple overlapping stents

Funding This study has received funding by National Natural Science Foundation of China (Grant No.: 81671678, 81671673) and Shanghai Municipal Education Commission-Gaofeng Clinical Medicine Grant Support (Grant No.: 20161428).

Compliance with ethical standards

Guarantor The scientific guarantor of this publication is Dr. Jiayin Zhang.

Conflict of interest The authors of this manuscript declare no relationships with any companies whose products or services may be related to the subject matter of the article.

Statistics and biometry No complex statistical methods were necessary for this paper.

Ethical approval Institutional review board approval was obtained.

Informed consent Written informed consent was obtained from all patients.

Methodology
- prospective
- diagnostic or prognostic study
- performed at one institution

References

1. Sousa JE, Serruys PW, Costa MA (2003) New frontiers in cardiology: drug-eluting stents: Part I. Circulation 107:2274–2279
2. Sousa JE, Serruys PW, Costa MA (2003) New frontiers in cardiology: drug-eluting stents: Part II. Circulation 107:2283–2289
3. Moses JW, Leon MB, Popma JJ et al (2003) Sirolimus-eluting stents versus standard stents in patients with stenosis in a native coronary artery. N Engl J Med 349:1315–1323
4. Stone GW, Ellis SG, Cox DA et al (2004) A polymer-based, paclitaxel-eluting stent in patients with coronary artery disease. N Engl J Med 350:221–231
5. Pan J, Lu Z, Zhang J et al (2013) Angiographic patterns of in-stent restenosis classified by computed tomography in patients with drug-eluting stents: correlation with invasive coronary angiography. Eur Radiol 23:101–107
6. Xu N, Zhang J, Li M et al (2014) Incidence and classification of neointimal proliferation and in-stent restenosis in post-stenting patients at 1-year interval: findings from non-invasive coronary computed tomography angiography. Eur J Radiol 83:1816–1821
7. Li M, Zhang J, Zhang Q et al (2015) Coronary stent occlusion: reverse attenuation gradient sign observed at computed tomography angiography improves diagnostic performance. Eur Radiol 25:568–574
8. Zhang J, Li M, Lu Z et al (2012) In vivo evaluation of stent patency by 64-slice multidetector CT coronary angiography: shall we do it or not? Int J Cardiovasc Imaging 28:651–658
9. Geyer LL, Glenn GR, De Cecco CN et al (2015) CT evaluation of small-diameter coronary artery stents: effect of an integrated circuit detector with iterative reconstruction. Radiology 276:706–714
10. Gassenmaier T, Petri N, Allmendinger T et al (2014) Next generation coronary CT angiography: in vitro evaluation of 27 coronary stents. Eur Radiol 24:2953–2961
11. Mangold S, Cannaó PM, Schoepf UJ et al (2016) Impact of an advanced image-based monoenergetic reconstruction algorithm on coronary stent visualization using third generation dual-source dual-energy CT: a phantom study. Eur Radiol 26:1871–1878
12. Maintz D, Seifarth H, Raupach R et al (2006) 64-slice multidetector coronary CT angiography: in vitro evaluation of 68 different stents. Eur Radiol 16:818–826
13. Ferencik M, Nomura CH, Maurovich-Horvat P et al (2006) Quantitative parameters of image quality in 64-slice computed tomography angiography of the coronary arteries. Eur J Radiol 57:373–379
14. Mehran R, Dangas G, Abizaid AS et al (1999) Angiographic patterns of in-stent restenosis: classification and implications for long-term outcome. Circulation 100:1872–1878
15. Tan SK, Yeong CH, Ng KH et al (2016) Recent update on radiation dose assessment for the state-of-the-art coronary computed tomography angiography protocols. PLoS One 11:e0161543
16. Stettler C, Wandel S, Allemann S et al (2007) Outcomes associated with drug-eluting and bare-metal stents: a collaborative network meta-analysis. Lancet 370:937–948
17. Rathore S, Kinoshita Y, Terashima M et al (2010) A comparison of clinical presentations, angiographic patterns and outcomes of in-stent restenosis between bare metal stents and drug eluting stents. EuroIntervention 5:841–846
18. Chen MS, John JM, Chew DP et al (2006) Bare metal stent restenosis is not a benign clinical entity. Am Heart J 151:1260–1264
19. Bossi I, Klersy C, Black AJ et al (2000) In-stent restenosis: long-term outcome and predictors of subsequent target lesion revascularization after repeat balloon angioplasty. J Am Coll Cardiol 35:1569–1576
20. Taylor AJ, Cerqueira M, Hodgson JM et al (2010) ACCF/SCCT/ACR/AHA/ASE/ASNC/NASCI/SCAI/SCMR 2010 appropriate use criteria for cardiac computed tomography. A report of the American College of Cardiology Foundation Appropriate Use Criteria Task Force, the Society of Cardiovascular Computed Tomography, the American College of Radiology, the American Heart Association, the American Society of Echocardiography, the American Society of Nuclear Cardiology, the North American Society for Cardiovascular Imaging, the Society for Cardiovascular Angiography and Interventions, and the Society for Cardiovascular Magnetic Resonance. J Am Coll Cardiol 56:1864–1894
21. Morsbach F, Desbiolles L, Plass A et al (2013) Stenosis quantification in coronary CT angiography: impact of an integrated circuit detector with iterative reconstruction. Invest Radiol 48:32–40